

BOND CHARACTERIZATION IN VERY HIGH POWER ULTRASONIC ADDITIVE MANUFACTURING

M.R. Sriraman*, Hiromichi Fujii*, Matt Gonser*, S.S. Babu*, and Matt Short[†]

*Department of Materials Science and Engineering, The Ohio State University, Columbus, OH 43221, USA

[†]Edison Welding Institute, Columbus, OH 43221, USA

Reviewed, accepted September 23, 2010

Abstract

Solid parts were produced by Very High Power Ultrasonic Additive Manufacturing (VHP-UAM) at room temperature using 150 μm thick tapes of 6061 aluminum and 110 copper alloys. Processing was done at 20 kHz frequency over a range of parameters (26–36 μm vibration amplitude, 5.6–6.7 kN normal force, and 30.5–35.5 mm/s travel speed). Softening of materials (up to about 14% in 6061 Al and 23% in 110 Cu) was noted facilitating enhanced plastic flow and a reduction in interfacial voids. Evolution of fine recrystallized grains (0.3–4 μm in 6061 Al and 0.3–10 μm in 110 Cu) from an initial coarser grain structure (up to 8 μm in 6061 Al and 25 μm in Cu) was observed at the build interface regions. Bonding between layers in both materials seems to have occurred by dynamic recrystallization and movement of grain boundaries across the interface. The energy required for the above physical processes is derived from interfacial adiabatic plastic deformation heating.

Introduction

Additive manufacturing is a set of manufacturing processes that involves the production of a 3-D part layer by layer directly from a CAD model [1]. Also known as layered manufacturing or rapid prototyping, this technology enables building of complex shaped parts that have hitherto been impossible by traditional means [1]. Ultrasonic Additive Manufacturing (UAM) is one such process used to fabricate parts of near net shape from metal tapes [2]. Based on ultrasonic seam welding, this solid state joining process involves successive bonding of metal tapes one over the other [3]. Ultrasonic vibrations (20 kHz frequency) are applied laterally to the foil through a sonotrode under a static normal force as the sonotrode rolls along the length of the tape. The scrubbing that takes place between the tapes ruptures the oxide layers between them, promoting nascent metal-metal contact and eventually their bonding. The sonotrode surface is usually textured to enable gripping of the foil and facilitate welding of the faying surfaces. This leaves a rough imprint on the top-surface of the tape. These imprints affect the bonding of the subsequent layer. The main process parameters for a given sonotrode texture are vibration amplitude, static normal force, sonotrode travel speed and pre-heat temperature [3].

A number of investigations have been carried out to characterize the bonding between metals in UAM [4-8]. Microstructural changes occurring under this process and the ensuing mechanical properties (hardness and strength) have been studied [4-11]. However, due to limited power capability of previous systems [12], adequate bonding has not been possible even in Al despite the pre-heat [3, 13]. This results in a large number of interfacial voids and discontinuities throughout the build [3, 13]. Furthermore, welding of materials harder than aluminum has not been possible. Preliminary attempts have been made to bond copper and some dissimilar metal combinations [6-7] with limited success. These shortcomings in the current UAM method have led to the development of very high power ultrasonic additive manufacturing (VHP-UAM). Such a process will involve higher ultrasonic power (or energy) realized through larger vibration

amplitudes and normal force levels. Such a VHP-UAM machine has been designed and developed by the EWI [12]. It is capable of delivering up to 9 kW of power at 20 kHz resonant frequency through the use of two transducers operating in tandem on either side of the sonotrode [12, 14]. A schematic of this is shown in Fig. 1. The two transducers are set to vibrate 180° out of phase, in “push-pull” mode. The transducer displacements are reinforced resulting in vibration amplitudes of up to 52 μm (from 26 μm in the conventional machine) [12]. In addition, the machine also has the capability for higher static normal forces – up to 15 kN [much higher than in the conventional machine (2 kN)] [12]. In this paper, 6061 Al (Al- 1% Mg, 0.6% Si, and 0.3% Cu by weight) [15] and 110 Electrolytic Tough Pitch Cu (99.95 % Cu and 0.04% O by weight) [15] have been processed by VHP-UAM. The bonds were then characterized by a variety of techniques.

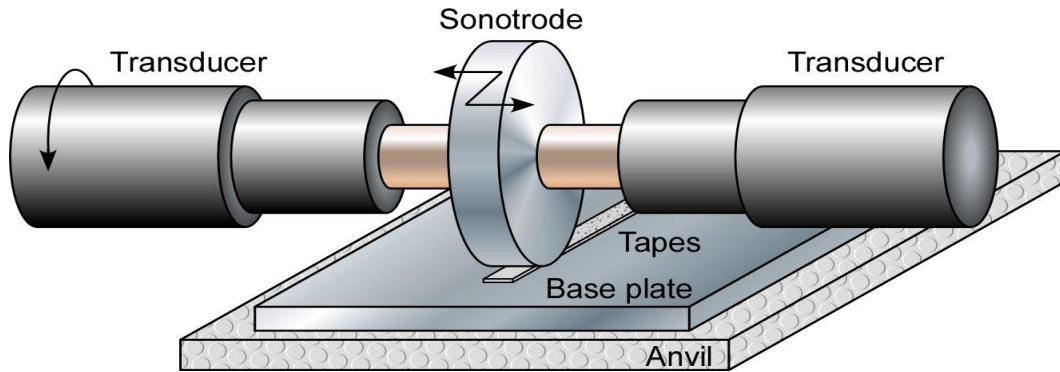


Fig. 1 Schematic of the double transducer-sonotrode system used in the VHP-UAM machine for enhanced vibration amplitudes.

Experimental Procedure

Separate builds of 6061 Al and 110 Cu were made by welding of tapes 150-μm thick successively one over the other. The first tape was always laid on (welded) to a 12-mm thick 3003Al-H14 base plate. The approximate dimensions of the builds were 25.4 mm width X 170 mm length X 2 mm height. Processing of materials was done at room temperature using the parameters shown in Table 1.

Table 1 VHP-UAM processing parameters used in the current investigations

Material	Vibration amplitude (μm)	Normal force (kN)	Travel speed (mm/s)
6061 Al-H18	26	5.6	35.5
110 Cu-Hard	36	6.7	30.5

The builds were characterized on transverse sections perpendicular to the welding direction. The samples were sectioned at low speed using a diamond blade and prepared in accordance with standard metallographic practice. They were then final polished with 0.02 μm colloidal silica on a vibratory polisher for ~36 hours. Optical microscopy and Scanning electron microscopy (SEM) (using the Quanta 200 Scanning electron microscope) were used to observe un-bonded regions and interfacial discontinuities. Microhardness mapping across the build (grid comprising of 31 rows spaced at 60 μm intervals and 20 columns spread over a length of about 20 mm) was done using a Leco AMH-43 Microhardness analyzer. The microstructure evolution

at the interface regions was investigated employing the technique of Orientation imaging microscopy (OIM) on Quanta 200 under the following conditions: 20-25 kV, spot size 6, 21-25 mm working distance, and 0.1-0.2 μm step size. For comparative studies, the original base material foils were also characterized on transverse sections.

Results and Discussion

6061 Aluminum Alloy Builds

Typical optical images from an as-polished 6061 Al build sample is shown in Fig. 2. The presence of a few voids is seen in the sample center (Fig. 2a) while relatively more voids are observed towards the edges (Fig. 2b). The void density is estimated to be 0.2 - 0.4% in a total area of 2 mm^2 . These un-bonded regions however are noticeably lower than what is typically seen in conventional UAM (Fig. 2c). Although the processing parameters used here are not optimal, the observation of a low void density indicates that improved bond quality is possible from the VHP process.

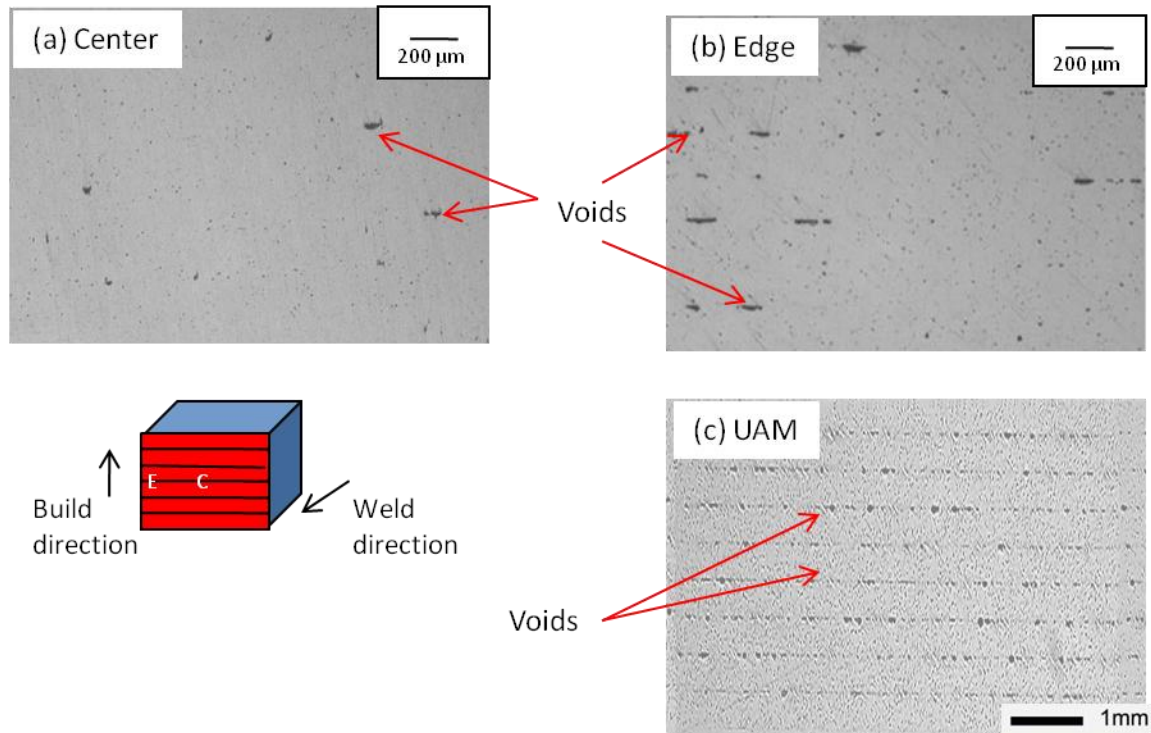


Fig. 2 Optical images of as-polished 6061 Al build sample (transverse section) showing (a) the void distribution in center and (b) edge. The optical image of the sample made by conventional UAM is shown in (c) for comparison [13]. A schematic of the transverse section showing regions corresponding to center and edge (denoted by C and E respectively) is also shown for reference.

The presence of more voids towards the edges could be attributed to a non-uniform contact pressure distribution at the interfacial region when a layer is bonded. Imprints of the sonotrode surface texture left on the foil (Fig. 3) show regions close to the edge of the tape (Fig. 3a) that are left “untouched” by the sonotrode surface. The tape center (Fig. 3b) on the contrary has a more uniform surface texture (Fig. 3b).

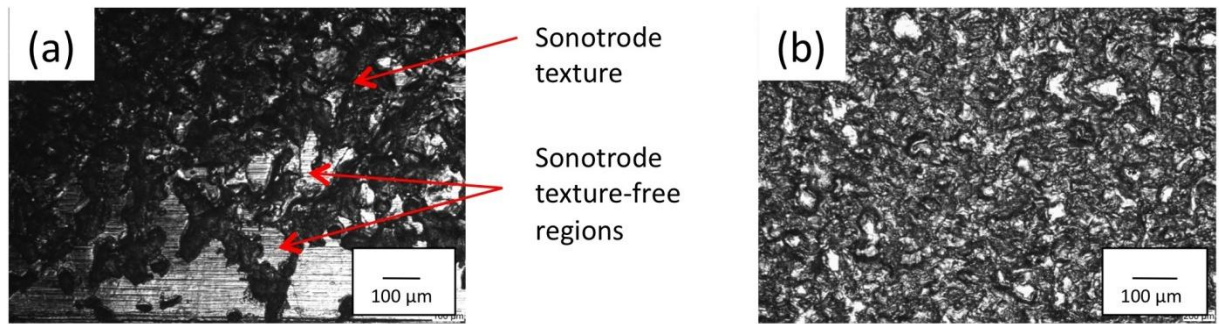


Fig. 3 Optical images of 6061 Al build top surface showing regions in the edge (a) where the sonotrode does not make contact unlike in the center (b).

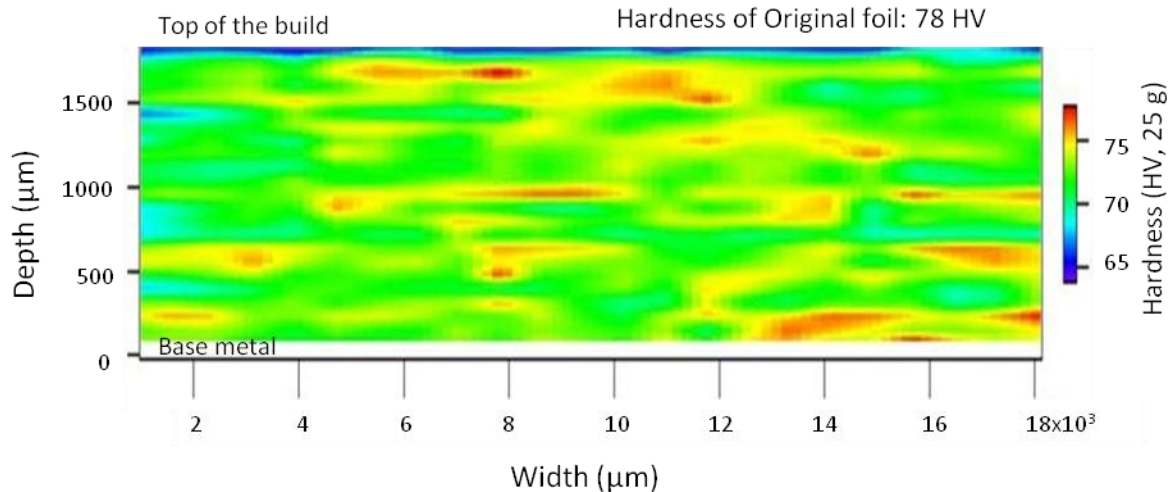


Fig. 4 Hardness map over the 6061 Al build sample showing a decrease in hardness in comparison to that of the original foil.

Microhardness measurements (Fig. 4) revealed softening of the material, at both the interface and bulk regions, in comparison to the hardness of original foil (78 HV). A hardness drop of up to ~14% is noted. However, as can be seen (Fig. 4), the extent of softening is not uniform across the build, with certain regions being almost as hard as the original foil. Such “hard” regions are found to be distributed throughout the build (Fig. 4). Although the reason for this is not clear, it is hypothesized that they could correspond to regions where plastic flow has not been homogeneous. Such inhomogeneous flow can arise from a non-uniform contact pressure distribution beneath the sonotrode [16]. Also, no specific trend is noticed with respect to the hardness variation either across the build height or along the transverse direction (Fig. 4).

Microstructure analysis shows the evolution of a fine equiaxed grain structure at the interface region (Fig. 5). Fig. 5b is an inverse pole figure (IPF) from one such region in the build sample. Regions of the same color signify those grains that have their corresponding crystallographic planes (indicated by the color triangle) oriented parallel to the sample surface.

The IPF of the original foil is shown in Fig. 5a. Although the confidence index has been rather low (0.14), the difference between the microstructures is clear. It is seen that a larger pancake shaped grain size distribution in the original foil (up to 8 μm) has been reduced to a finer equiaxed grain structure (0.3-4 μm) at the interface region following bonding (Fig. 5c). The finer grain structure that is evolved during processing also has a larger fraction of grain boundaries with high angle misorientations (15-65 $^\circ$) between them (Fig. 5d). The formation of such fine equiaxed grains with large misorientations suggests the occurrence of recrystallization. Since the interface is not distinctly visible (Fig. 5a), the grain boundaries (of recrystallized grains) must have moved across the interface, leading to metallurgical bonding.

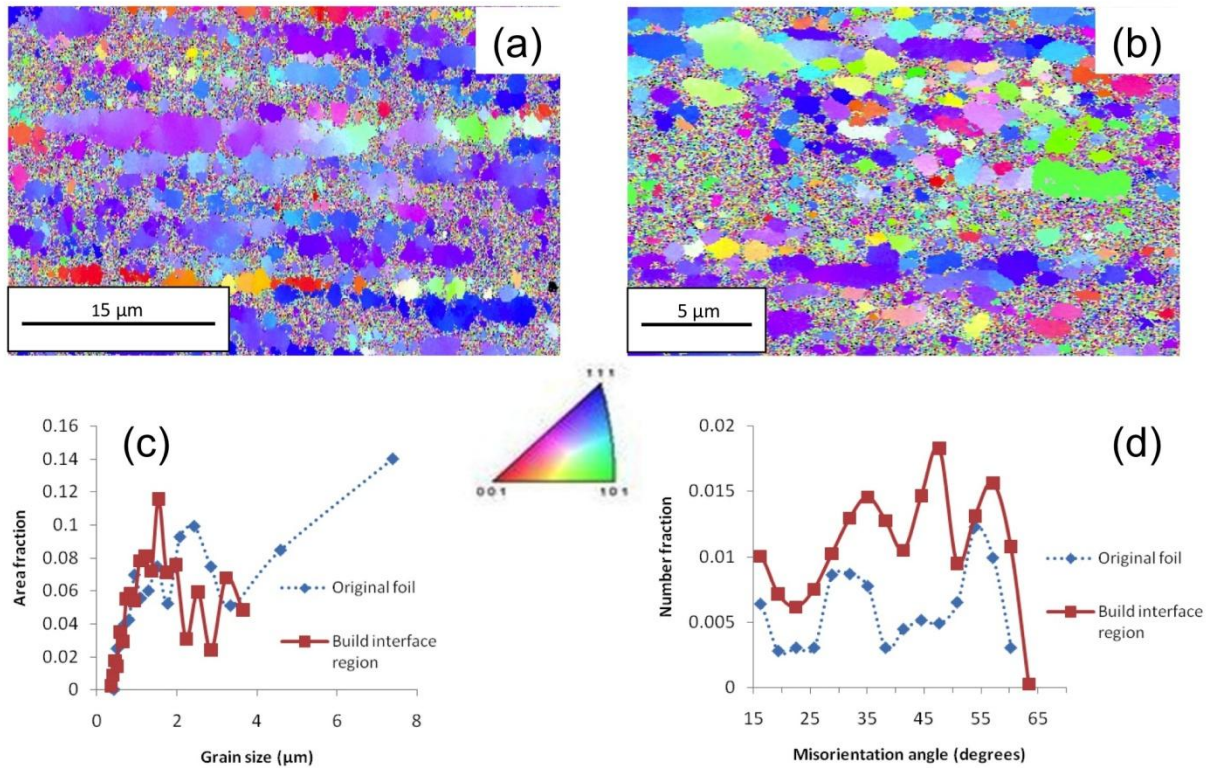


Fig. 5 Inverse pole figures of (a) the original 6061 Al foil and (b) an interface region from the build. Analyses of the data shows (c) finer grain size distribution and (d) larger grain misorientations at the build interface.

A clear change in the crystallographic texture is also noted as seen from the (111) pole figures (Fig. 6). The original foil (Fig. 6a) shows a typical $\{112\} \langle 111 \rangle$ “copper” texture that is commonly observed with heavily cold rolled face centered cubic metals [17]. The interface region however seems to display a weak “cube” texture ($\{001\} \langle 100 \rangle$) [17] again pointing to recrystallization of the initial deformed structure. This is shown in Fig. 6b. Recrystallization has been observed earlier in conventional UAM of Al (3003 alloy) [3, 18]. In the current investigations however, the phenomenon observed can only be attributed to dynamic recrystallization (DRX) since no external heating is involved. DRX signifies recrystallization of grains even as it is being deformed. Such a phenomenon has also been reported in conventional

UAM of 6061-O Al done without pre-heat [10]. The occurrence of DRX probably explains the softening seen in our investigations.

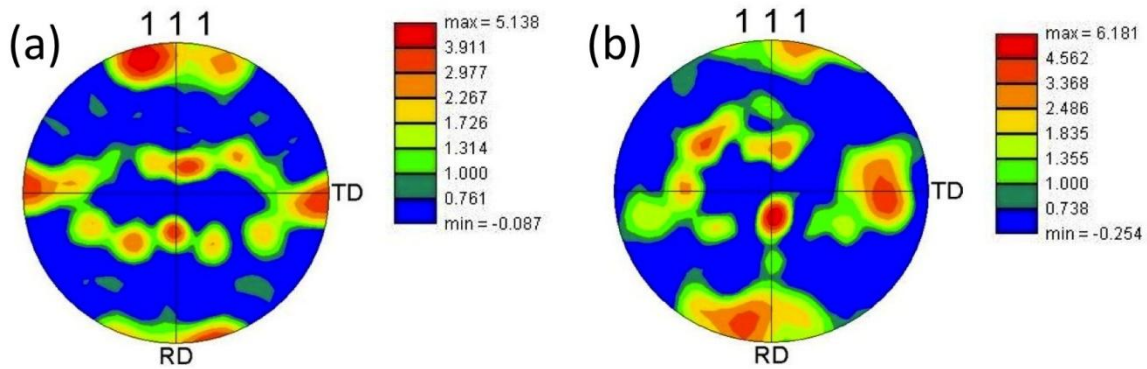


Fig. 6 (111) Pole figures of (a) the original 6061 Al foil and (b) an interface region of the build sample showing a weak cube texture evolution in the interface from an initial copper texture.

110 Cu Alloy Builds

Bonding in 110 Cu is seen to comprise of the formation of wavy interfaces with evidence of turbulent plastic flow in certain regions (Fig. 7). The presence of such interfacial instabilities was clearly brought out in the etched build sample under the SEM (Fig. 7). This could be an effect of the material flow occurring along the ridges and valleys between the contacting layers during processing. The wavy nature of interfaces is probably connected with the ability of copper to work soften and flow easily (than Al) with increasing temperatures, due to its lower stacking fault energy (SFE) [19-21]. It is also apparent (Fig. 7) that the tapes had individually thinned down by about 5% from the original thickness of 150 μm .

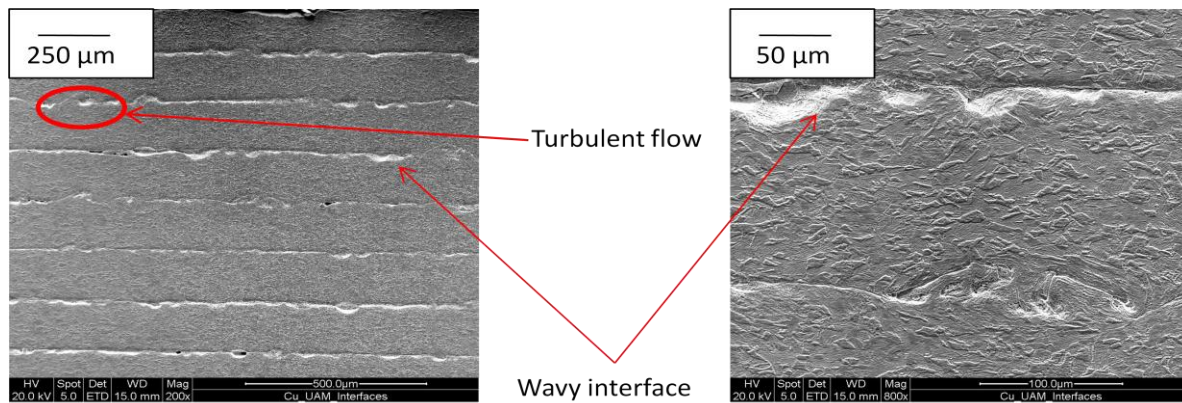


Fig. 7 Secondary electron images of 110 Cu build sample etched with 50% nitric acid.

Softening of the material throughout the build (even greater than in 6061 Al) is observed here again. Fig. 8 shows the hardness map over the build sample. In comparison with a harder original foil material (108 HV), the build layers are seen to have softened up to ~23% (Fig. 8). However, there are some “hard” regions as well. Again, no specific trend is seen in the hardness variation along the build height or in the transverse direction (Fig. 8).

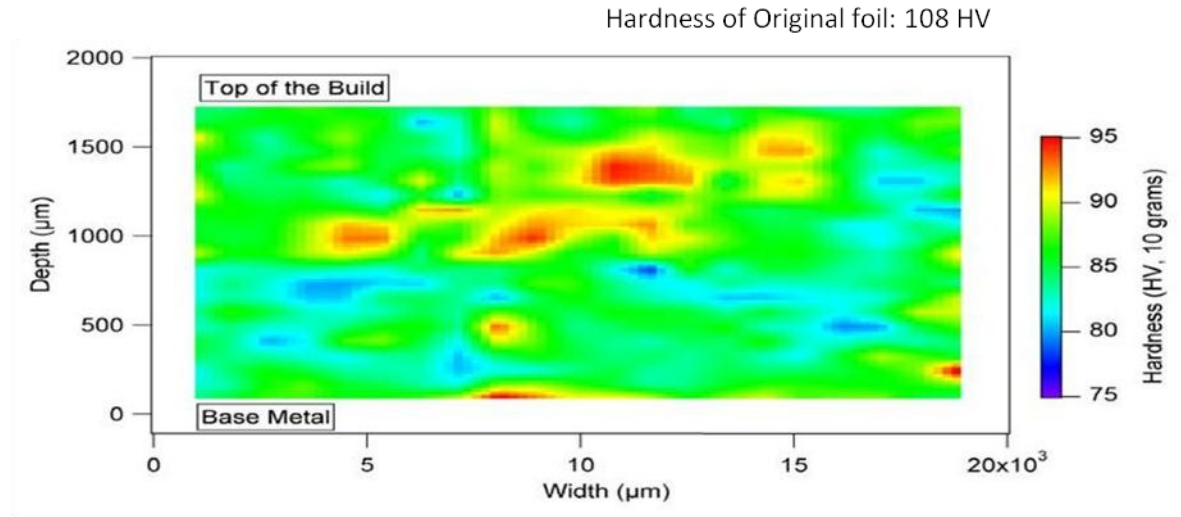


Fig. 8 Hardness map over the 110 Cu build sample showing a decrease in hardness in comparison with the original foil.

The evolution of a fine equiaxed grain structure at the interface region was again noted (Fig. 9). Figures 9a and 9b show the IPF of the original foil and an interface region in the build sample. The difference between the two images (Figs. 9a and b) is striking with the latter showing evidence of highly localized shear (Fig. 9b). Grain size analysis reveals that a relatively coarse grain structure of up to 25 μm size in the as-received foil is reduced on processing to a more uniformly finer grain size ranging between 0.3-10 μm (Fig. 9c). This fine grain structure in the interface region also contains a larger fraction of grains with high angle misorientations (15-60°) between them than the original foil (Fig. 9d) pointing once again to recrystallization and consequent metallurgical bonding. Again, with no external heating involved in the processing of the build, the evolved grain structure at the interface region could be attributed only to DRX. It is probably the first time this phenomenon is being observed in UAM of Cu. A change in texture is seen here too - between the original foil and the interface region of the build - as seen in the (111) pole figures (Fig. 10). It is interesting to note that a deformation texture (copper type) seems to evolve following processing (Fig. 10b). This could be associated with the shearing seen therein (Fig. 9b) and is being further investigated.

With the observation of dynamic recrystallization occurring in both materials at the interface, it appears the starting cold worked coarse grain structure of the original foils has gone through the stages of further plastic deformation (expected to be more in Cu due to its high work hardening rate) and dynamic recovery (in Al) during VHP-UAM. Al alloys, with their high SFE, are known to exhibit continuous dynamic recrystallization (CDRX) [10, 22] especially under hot working/ thermomechanical processing [19-21] where the subgrains undergo a continuous rotation until they form high angle boundaries between them [10, 22]. Copper, on the other hand, being a material with medium SFE, is known to exhibit discontinuous dynamic recrystallization (DDRX) under hot working conditions [23]. This involves the nucleation of grains with high angle misorientation with the parent grains [23].

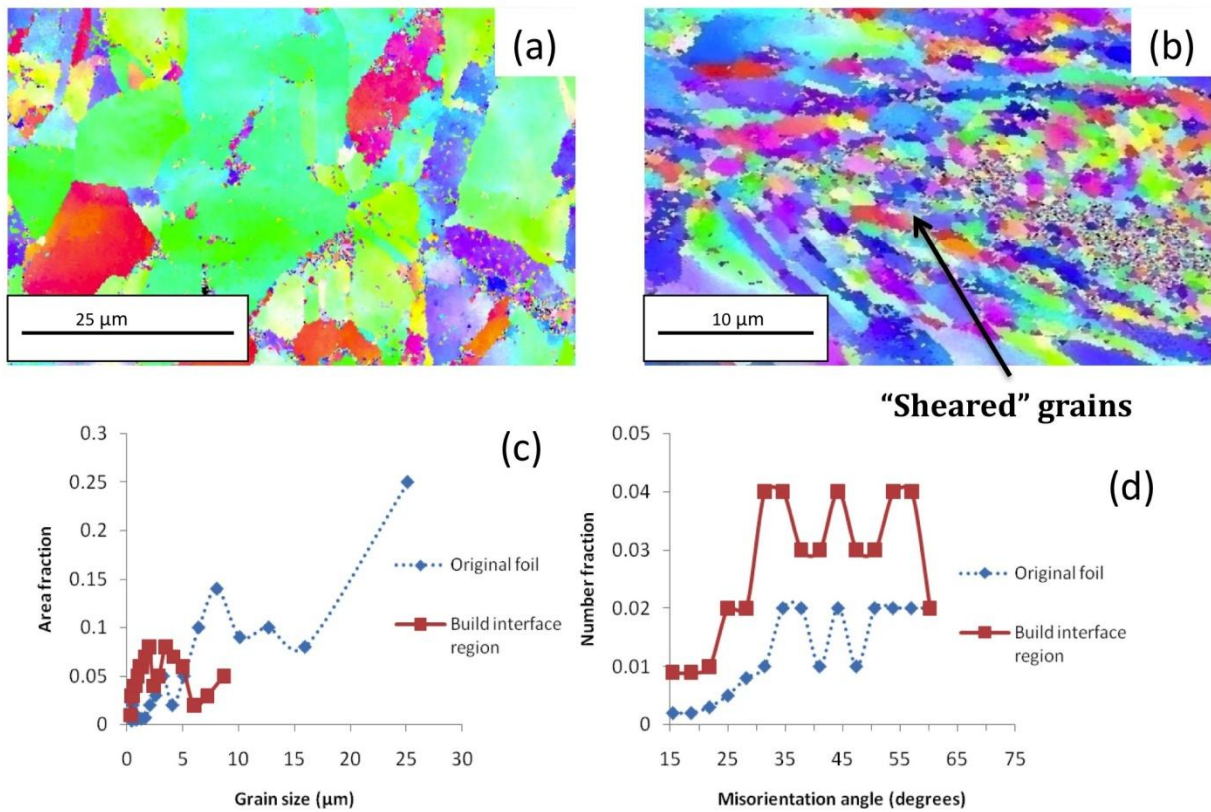


Fig. 9 Inverse pole figures from (a) the original 110 Cu foil and (b) an interface region in the build sample. Analyses of the data shows (c) finer grain size distribution and (d) larger grain misorientations at the build interface.

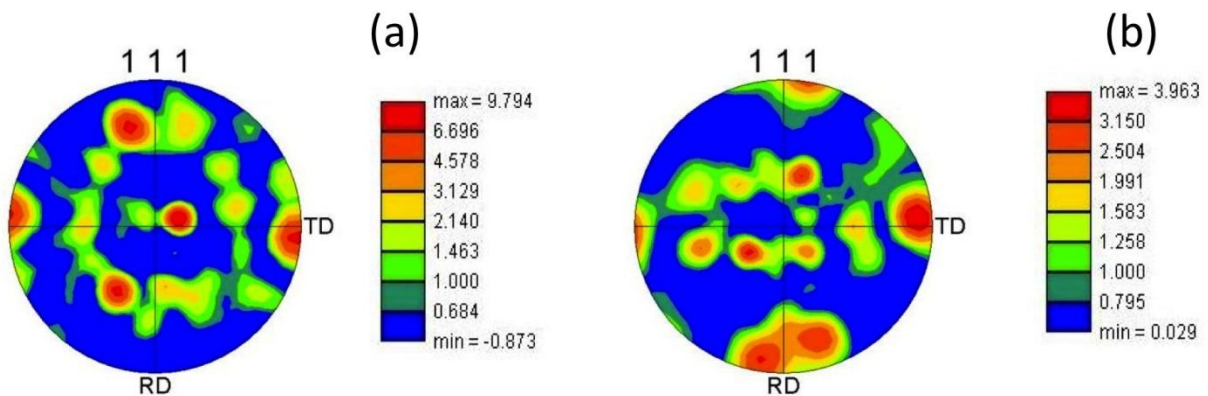


Fig. 10 (111) Pole figures of (a) the original 110 Cu foil and (b) an interface region of the build sample showing the possible evolution of a copper texture at the interface region.

The occurrence of recrystallization suggests that the interfacial temperature during the process must have reached close to the homologous temperature of 0.5 (although in Al alloys, the temperature could be lower) [19]. It is further interesting to note that this might have actually

occurred within a few milliseconds only [24] entirely due to interfacial heating. The evolution of recrystallized grains at the interface explains the softening observed in both materials. The heat generated at the interface could also get dissipated into the bulk. Since the starting material is in the cold rolled condition, such heat dissipation could lead to recovery-like effects in the bulk of the layers [25]. This probably explains the softening through the thickness of the layers.

Since the process involves shearing of small micron sized asperities between the foils at a frequency of 20 kHz and high vibration amplitudes, very high strains and strain rates can develop. Strain rate estimates under ultrasonic welding/ UAM point to a figure as high as $10^4 - 10^5 \text{ s}^{-1}$ [7, 26]. This could result in high strain rate deformation heating under adiabatic conditions resulting in large temperature excursions [27-28]. The flow stress of the material is thus decreased appreciably even as the high strain rate tries to increase it [20]. Between these competing processes, the effect of temperature eventually prevails resulting in work softening through dynamic recovery (DRV) and/or recrystallization (DRX) [17, 20-21]. Such a behavior can induce plastic instability in the material promoting enhanced flow, more so in materials with relatively lower SFE [17, 21]. This is probably the reason for the turbulent flow in Cu. Such inducement of enhanced plastic flow can result in a more effective collapse of asperities too. This would minimize voids and un-bonded regions, as was noted in this research. A further reduction in void density (than reported here) was also seen to be possible under VHP processing (as part of our overall research program) [25]. Temperature rise estimates made based on adiabatic heating during metal working show that the excursions in temperature over every cycle can indeed be large and close to a homologous temperature of 0.5 [24]. VHP-UAM can thus be compared to hot working (albeit in a much localized fashion) where such temperatures are involved promoting DRX [19].

Based on the above, the following bonding mechanism is hypothesized in VHP-UAM:

1. Scrubbing of layers leading to oxide film rupture between all contacting asperities, their delamination, and dispersion - due to differential deformation characteristics between the oxide and the metal.
2. Contact of nascent metal asperities, their interfacial cyclic shearing and strain hardening.
3. Formation of hysteresis loops, plastic deformation heating under adiabatic conditions due to high strain rates.
4. Rapid localized temperature rise with every cycle together with plastic strain accumulation.
5. Softening by DRV/ DRX and decrease in flow stress and modulus of the interfacial metal.
6. Enhanced plastic flow, asperity “collapse”, and further softening.
7. Mutual migration of boundaries of recrystallized grains across the interface.
8. Formation of a series of “micro welds”.

Although listed sequentially, these stages in bonding could occur concurrently. For instance, the initial plastic deformation cycles could lead to adiabatic heating conditions, which in turn facilitate more plastic flow. Again, the softening that takes place by the mechanism of DRV/ DRX could promote more plastic flow and a possible further softening due to continued heating. Also, even as the contacting asperities collapse against each other, new asperities start coming into contact as the cycle repeats itself.

In order to test the above hypothesis of plastic deformation heating being the driver to DRV/ DRX in VHP-UAM, some temperature measurements using K type thermocouples were made in Al alloys (3003, 6061) and 110 Cu [29]. A higher temperature rise was recorded in the higher strength materials namely 6061 Al and 110 Cu in comparison with 3003 Al under similar processing conditions [29] demonstrating the effect of plastic deformation heating. The observations also fit into the phenomenological model of adiabatic temperature rise due to plastic work [24]. Based on the above mechanism, bonding in a given material must also depend upon the energy that is put in through the processing parameters. This input energy will in turn determine the extent of temperature rise at the interface promoting bonding through the mechanism discussed. This phenomenon was again verified by temperature measurements in 3003 Al [29]. Although all the three parameters - vibration amplitude, normal force, and travel speed were found to influence the temperature rise [29], the effect of amplitude was the most pronounced [29]. These results also agree with the phenomenological model [24]. According to the model, the temperature rise will be a function of the shear strain associated with plastic work. Since the shear strain is proportional to the amplitude [24], higher the amplitude, larger will be the temperature increase. The results [29] of increased temperature rise with amplitude (in 3003 Al) corroborates with observations made earlier [14]. A higher degree of bonding, as assessed by qualitative peel testing, was noted under increased amplitudes [14].

Future work would involve mechanical testing of VHP-UAM builds to evaluate the “bond strengths” and identify optimal processing parameters for a given material. This would confirm the above hypothesis of temperature rise being a measure to the bond quality. Also, it would be interesting and important to observe the microstructural evolution away from the interfaces to rationalize the softening in the bulk.

Conclusions

Multilayer builds of 6061 Al and 110 Cu were made by very high power ultrasonic additive manufacturing at room temperature. With enhanced plastic flow facilitated through more intense processing parameters than in conventional ultrasonic additive manufacturing, voids/ unbonded regions are significantly low (only about 0.2-0.4% in 6061 Al over 2 mm²). Wavy interfaces with features of turbulent plastic flow are noticed in 110 Cu. Bonding in both materials is seen to take place through the process of dynamic recrystallization and a possible migration of grain boundaries across the interface. While the grain structure in 6061 Al is reduced to 0.3-4 μm from an initial starting foil grain size of up to 8 μm, it is refined to 0.3-10 μm from a grain size of up to 25 μm in the starting foil. This is accompanied by a change in crystallographic texture too at the interface region. Softening of materials from the original foil hardness is also observed (up to about 14% in 6061 Al and 23% in 110 Cu). This is probably responsible for the enhanced flow. The differences in the extent of softening between 6061 Al and 110 Cu could be attributed to the difference in their stacking fault energies. The temperature rise promoting dynamic recrystallization during bonding seems to occur through plastic deformation heating between contacting asperities. The above results illustrate the potential benefit of VHP-UAM.

Acknowledgements

The authors are thankful to the Ohio department of development for funding this research work through the Third frontier Wright Projects program. The guidance and support received from Dr.

Karl Graff of EWI throughout this research is greatly appreciated. Kind assistance from the staff/ students of EWI/ OSU is also gratefully acknowledged.

References

- [1] Xiaochun Li, Hongseok Choi, Yong Yang, *Thin Solid Films* 420-421 (2002) 515.
- [2] Dawn R. White, *Advanced Materials and Processes* (2003) 64.
- [3] D. Schick, R. Hahnen, R. Dehoff, S. S. Babu, P. Collins, M. Dapino, J. C. Lippold, *Welding Journal*, 89 (2010) 105.
- [4] C.Y. Kong, R.C. Soar, P.M. Dickens, *J. Mat. Proc. Tech.* 146 (2004) 181.
- [5] C.Y. Kong, R.C. Soar, P.M. Dickens, *Materials Science and Engineering A363* (2003) 99.
- [6] Ken Johnson, *Proc. of The Second Symposium on Ultrasonic Additive Manufacturing*, Edison Welding Institute, Columbus, Ohio, Oct. 20-21, 2009.
- [7] Y. Yang, G.D. Janaki Ram, B.E. Stucker, *J. Mater. Proc. Tech.* 209 (2009) 4915.
- [8] Brent L. Adams, Clayton Nylander, Brady Aydelotte, Sadegh Ahmadi, Colin Landon, Brent E. Stucker, G.D. Janaki Ram, *Acta Materialia* 56 (2008) 128.
- [9] Dezhi Li, Rupert C. Soar, *Materials Science and Engineering A* 498 (2008) 421.
- [10] E. Mariani, E. Ghassemieh, *Acta Materialia* 58 (2010) 2492.
- [11] C.Y. Kong, R.C. Soar, P.M. Dickens, *J. Mechanical Engineering Science* 219 (2005) 83.
- [12] K. Graff, Edison Welding Institute, Private communication.
- [13] S. S. Babu, O. Barabash, and K. Graff Unpublished work, 2010.
- [14] M.R. Sriraman et al, *Proc. of The Second Symposium on Ultrasonic Additive Manufacturing*, Edison Welding Institute, Columbus, Ohio, Oct. 20-21, 2009.
- [15] Peter Robinson, *Properties of wrought Cu and alloys*, ASM Handbook Online, Vol. 2. (<http://products.asminternational.org/hbk/index.jsp>).
- [16] M. Kukalov and H.J. Rack, *J. Eng. Mat. Tech.* 131 (2009) 021006-1.
- [17] F.J. Humphreys and M. Hatherly, *Recrystallization and related annealing phenomena*, Pergamon, 1995.
- [18] R.R. Dehoff, S.S. Babu, To be published in *Acta Materialia*, 2010.
- [19] Y.V.R.K. Prasad, N. Ravichandran, *Bull. Mater. Sci.* 14 (1991) 1241.
- [20] G.E. Dieter, *Mechanical metallurgy*, McGraw-Hill, 1986.
- [21] S.L. Semiatin and J.J. Jonas, *Formability and workability of metals*, ASM, 1984.
- [22] K.V. Jata, S.L. Semiatin, *Scripta Materialia* 43 (2000) 743.
- [23] M. El Wahabi, L. Gavard, F. Montheillet, J.M. Cabrera, J.M. Prado, *Acta Materialia*, 53 (2005) 4605.
- [24] M.R. Sriraman, S.S. Babu, and M. Short, *Scripta Materialia*, 62 (2010) 560.
- [25] K. Sojiphan, M.R. Sriraman, S.S. Babu, Paper to be presented in Twenty First Annual International Solid Freeform Fabrication Symposium – An Additive Manufacturing Conference, Aug. 9-11, Austin, Texas, USA.
- [26] I.E. Gunduz, T. Ando, E. Shattuck, P.Y. Wong, C. Dourmanidis, *Scripta Materialia* 52 (2005) 939.
- [27] M.A. Meyers, J.C. LaSalvia, V.F. Nestorenko, Y.J. Chen, B.K. Kad, *Proc. of The Third International Conference on Recrystallization and Related Phenomena (ReX '96)*, Ed: Terry R. McNelley, 1996, pp. 279-286.
- [28] U. Andrade, M.A. Meyers, K.S. Vecchio, A.H. Chokshi, *Acta Metall. Mater.* 42 (1994) 3183.
- [29] M.R. Sriraman, Matthew Gonser, Hiromichi Fujii, S.S. Babu, Matt Bloss, Unpublished work, 2010.